International Immunopharmacology 71 (2019) 188–197

Contents lists available at ScienceDirect

International Immunopharmacology

journal homepage: www.elsevier.com/locate/intimp

Inhibition of the TIRAP-c-Jun interaction as a therapeutic strategy for AP1-mediated inflammatory responses

Mansi Srivastava[a,1], Uzma Saqib[b,1], Sreeparna Banerjee[c], Kishore Wary[d], Burak Kizil[c], Kannan Muthu[e], Mirza S. Baig[a,*]

[a] Discipline of Biosciences and Biomedical Engineering (BSBE), Indian Institute of Technology Indore (IITI), Simrol, 453552 Indore, MP, India
[b] Discipline of Chemistry, School of Basic Sciences, Indian Institute of Technology Indore (IITI), Simrol, 453552 Indore, MP, India
[c] Department of Biological Sciences, Orta Doğu Teknik Üniversitesi (ODTÜ), Ankara 06800, Turkey
[d] Department of Pharmacology, University of Illinois at Chicago, Chicago, IL 60612, USA
[e] Department of Crystallography and Biophysics, University of Madras, Guindy Campus, Chennai, 600025, TN, India

ARTICLE INFO

Keywords:
Inflammation
Macrophage
Activator protein-1 (AP-1)
Proinflammatory cytokines
c-Jun
TIRAP

ABSTRACT

Bacterial endotoxin-induced sepsis causes 30–40% of the deaths in the intensive care unit (ICU) globally, for which there is no pharmacotherapy. Lipopolysaccharide (LPS), a bacterial endotoxin, stimulates the Toll-like receptor (TLR)-4 signalling pathways to upregulate the expression of various inflammatory mediators. Here, we show that the TIRAP and c-Jun protein signalling complex forms in macrophages in response to LPS stimulation, which increases the AP1 transcriptional activity, thereby amplifying the expression of inflammatory mediators. Using a computer-aided molecular docking platform, we identified gefitinib as a putative inhibitor of the TIRAP-c-Jun signalling complex.

Further, we demonstrated the ability of gefitinib to inhibit the interaction of TIRAP-c-Jun with in vitro experiments and with a mouse model of sepsis. Importantly, pre-treatment with gefitinib increased the survival of the mice that received a lethal dose of LPS compared to that of the controls. These findings verify the ability of gefitinib to directly disrupt the interaction of TIRAP and c-Jun, thereby inhibiting a major inflammatory response that is often observed in patients experiencing sepsis.

1. Introduction

The role of Toll-like receptors (TLRs) in inflammation and their ability to recognize microbial products has been well characterized [1–3]. Toll-like receptors (TLRs) recognize and react to both pathogen-associated molecular patterns and endogenous signals [4,5]. Except for TLR3, all TLRs recruit MyD88 to their receptor complex, after which MyD88 recruits interleukin-1 receptor-associated kinase 1 (IRAK1) and IRAK4; then, TNF receptor-associated factor 6 (TRAF6) is recruited, which results in the nuclear translocation of inflammatory transcription factors such as NF-κB and AP1 [6–10]. Although TLRs induce common signalling pathways, there is specificity in the recruitment of the TIR-containing adapter proteins.

TIRAP/Mal and TRAM have been described as bridging adapters that are responsible for the specific recruitment of MyD88 and TRIF proximal to the surface-localized TLR2 and TLR4 receptor complexes [11–14]. TIRAP acts as a bridge for MyD88 to TLR2 and TLR4, specifically via its TIR domain [12]. Inflammatory responses are aided by adaptor proteins such as TIRAP (Toll/interleukin-1 receptor domain-containing adapter protein) [14,15]. TIRAP potentiates signalling by allowing the activation of downstream kinases, which in turn activate the critical transcription factors NF-κB/AP1 that bind to and regulate proinflammatory cytokine gene expression [11,16]. To provide an adequate inflammatory response, TIRAP undergoes polyubiquitin-mediated degradation by SOCS1 after its phosphorylation by Bruton's tyrosine kinase (BTK) [17,18]. However, a recent study suggested that SOCS1 ubiquitination and proteasomal degradation occur after nitrosation by NOS1, implying that NOS1 negatively regulates SOCS1, therefore allowing the prolonged activation of the adapter protein TIRAP [19]. The presence of TIRAP in activated macrophages allows the transduction of the downstream signalling cascade. The activator protein-1 (AP1) transcription factor belongs to a family of leucine zipper-containing proteins and mediates signalling that arises through the activated TLR4 receptor [20,21]. Studies of the structural aspects of

* Corresponding author.
E-mail address: msb@iiti.ac.in (M.S. Baig).
[1] Contributed equally.

https://doi.org/10.1016/j.intimp.2019.03.031
Received 10 January 2019; Received in revised form 17 March 2019; Accepted 18 March 2019
Available online 22 March 2019

the AP1 transcription factor have provided insight into the three active subunits of AP1, Fos, c-Jun, and ATF2; among these proteins, c-Jun can heterodimerize with either Fos or ATF2 [22–25]. Active Fos-c-Jun or c-Jun-ATF2 dimers then translocate into the nucleus and bind to the target inflammatory genes regulating their expression [26,27]. This study provides mechanistic insight into the TIRAP-mediated transactivation of c-Jun that can facilitate the AP1 inflammatory responses. Briefly, LPS-induced endotoxin shock activates Bruton's tyrosine kinase (BTK), which phosphorylates the TIRAP molecule. Subsequently, TIRAP interacts with c-Jun and facilitates its transactivation. The activated c-Jun dimerizes with AP1 subunits (Fos and ATF2) and translocates into the nucleus to regulate the expression of the AP1 target genes. The endotoxin shock that is induced with LPS leads to elevated levels of proinflammatory cytokines, such as IL-12, IL-23, IFN-γ and MIP1-α, which activate the inflammatory cascade in immune cells.

Through a molecular docking analysis platform, we identified gefitinib, vemurafenib, cobicistat, empagliflozin, and canagliflozin as potential inhibitors of the TIRAP and c-Jun signalling complex. Accordingly, gefitinib inhibited the proinflammatory cytokine response to LPS-mediated TLR4 stimulation in macrophages by interfering with the formation of the TIRAP-c-Jun complex, thereby inhibiting the downstream activation of the AP1 transcriptional machinery. Furthermore, we identified the structural determinants of the TIRAP-c-Jun-gefitinib inhibitory complex that disrupt LPS-mediated TLR4 stimulation, thus delineating a novel role for gefitinib based on its ability to downregulate the inflammatory response to TLR4 activation on myeloid cells in vitro and in a mouse model of sepsis.

2. Materials and methods

2.1. Murine model

Swiss albino mice were acquired from the Veterinary College in Mhow and were housed at the animal house facility at Acropolis College. We used 8- to 12-week-old male mice, each weighing 28–30 g. The animal study was approved by the Institutional Animal Ethics Committee (IAEC) of the Acropolis Institute of Pharmaceutical Education and Research and was conducted in accordance with the policies of the Committee for the Purpose of Control and Supervision of Experiments on Animals (CPCSEA) of the Govt. of India. Mice were kept in a pathogen-free vivarium at a temperature of 20–25 °C and relative humidity (55–60%) with a 14:10 h light and dark cycle and had access to purified drinking water and a regular chow diet.

2.2. Cell culture

Bone marrow-derived macrophages (BMDMs) were collected from wild-type Swiss albino mice. Bones were collected in cold 1× sterile PBS and were cut at both ends to flush the bone marrow cells. BMDMs were cultured in DMEM (HiMedia) containing 10% heat-inactivated foetal bovine serum (Life Technologies), 100 U/ml penicillin and 100 g/ml streptomycin (Invitrogen, California, USA), along with 20% L929-cell conditioned media as a source of M-CSF for 72 h. Fresh media was exchanged after the third day of culture, containing 10% L929-cell conditioned media. Cell growth was synchronized by culturing with serum-free DMEM overnight. Fresh DMEM media with 10% FBS was added to the differentiated macrophages. Cells were incubated in a humidified incubator with 5% CO_2 at 37 °C.

2.3. Quantitative real-time PCR

Total mRNA was prepared from BMDMs using TRIzol reagent (Takara, Shiga, Japan) according to the manufacturer's instructions. cDNA was synthesized using a cDNA synthesis kit (Bio-Rad), followed by qPCR using SYBR Green PCR Master Mix (Applied Biosystems, Austin, USA). Ct values of the target gene were compared to that of the housekeeping gene (GAPDH) to quantify the gene expression in each sample. The primers used for the study are listed in Supplementary Table 1.

2.4. Co-immunoprecipitation and immunoblotting

Cells were stimulated with LPS (250 ng/ml) or gefitinib (1 μM) and were lysed in RIPA buffer (Life Technologies, Rockford, USA) diluted with a Tris–HCl base buffer (pH 7.5). Protein concentration was determined using a Bradford reagent (Biorad). A total of 250 ng of protein per sample was incubated with either TIRAP (sc-31309, Santa Cruz, California, USA) or c-Jun (sc-74543, Santa Cruz, California, USA) antibody overnight at 4 °C on a shaker. The next day, the protein-antibody complex was washed in base buffer and incubated with protein A/G plus-agarose beads (sc-2003, Cell Signaling Technology, California, USA) for 1 h at room temperature on a shaker. Antibody-bound proteins were pulled down along with the beads by centrifugation at 6000 rpm at 4 °C. Subsequently, the protein-antibody complex bound to the beads was immunoblotted with an antibody for either TIRAP or c-Jun.

For immunoblotting, cells were lysed in RIPA buffer (Life Technologies) containing protease and phosphatase inhibitor tablets (Invitrogen). Protein was resolved on 10% SDS-PAGE gels, blotted onto nitrocellulose membranes and probed with antibodies for TIRAP, c-Jun, and β-actin, followed by HRP-conjugated secondary antibody (anti-rabbit and anti-mouse) for visualization. All antibodies were obtained from Santa Cruz.

2.5. Confocal microscopy

BMDMs were seeded on coverslips in six-well plates. To initiate macrophage activation, cells were exposed to LPS (250 ng/ml) for 1 h. For confocal analysis, cells were washed with 1× PBS, fixed with 4% paraformaldehyde for 15 min at room temperature and permeabilized with 0.1% Triton X-100 for 10 min. Cells were then blocked with 5% BSA in 1× PBS for 1 h at room temperature. Primary antibodies for TIRAP and c-Jun were then added to the cells for 1 h (1:400). Following this incubation, the cells were stained with FITC-conjugated donkey anti-mouse or Alexa Fluor 594-conjugated goat anti-rabbit secondary antibodies for 1 h at room temperature. Nuclear counterstaining was carried out using DAPI mounting media (Thermo Fisher Scientific, Cat. No. 62248, Thermo Fisher Scientific, Germany) according to the manufacturer's instructions. Stained cells were analysed using an Olympus confocal laser scanning microscope.

2.6. In vivo study

To determine the therapeutic efficacy of gefitinib in murine septic models, mice were acclimatized in the animal house facility at Acropolis College in Indore in a pathogen-free vivarium and segregated randomly into five groups (two control and three experimental groups) with seven mice in each group. Briefly, gefitinib (Cat. No. A10422-100, Adooq Biosciences, Irvine, USA) was dissolved in a 1:9 solution of DMSO and 1× PBS. Gefitinib solution (40 mg/kg body weight of mice, 0.5 ml solution per mouse) was intraperitoneally injected into all mice. Two control groups were assigned, one without any injection, while the second group received a solvent injection (0.5 ml of 1:9 ratio of DMSO and 1× PBS). One hour after the gefitinib administration, LPS (*E. coli* B100) diluted in 0.5 ml of 1× PBS was intraperitoneally injected into the experimental mice (30 mg/kg body weight). Mortality of mice was noted for the experimental versus control mice for up to 72 h. Mice that survived the endotoxin shock were euthanized by CO_2 followed by cervical dislocation. Left and right lung lobes were harvested for haematoxylin and eosin (H&E) staining or for immunohistochemistry with antibodies for TIRAP and c-Jun.

2.7. Immunohistochemistry

The methods for immunohistochemistry have been previously described[1]. In brief, paraffin-embedded, thin (6–8 μm) lung sections were incubated in xylene for 15 min at room temperature. Post-xylene incubation, the sections were transferred to 100% ethanol for 15 min, followed by an incubation in 95%, 70% and 50% ethanol for 5 min each. Subsequently, each section was boiled to 90 °C for 10 min in Tris-EDTA (pH 9.0). The sections were then blocked in 3% BSA in TBST for 30 min at room temperature. Staining with a primary antibody (TIRAP and c-Jun; 1:400) was carried out for 1 h, followed by staining with FITC-conjugated donkey anti-mouse and Alexa Fluor 594-conjugated goat anti-rabbit secondary antibodies for 1 h at room temperature. Lung sections were mounted using DAPI mounting media (Sigma). Stained sections were visualized with an Olympus confocal laser scanning microscope.

2.8. Molecular modelling

The three-dimensional (3D) structure of c-Jun (residues 201 to 256) was modelled utilizing the Modbase program [28]. The structure of pre-mRNA-processing-splicing factor 8 (4KIT; Chain C) from the Protein Data Bank (PDB) was used as our template. The resulting model was minimized and subjected to molecular docking with TIRAP. The crystal structure of the TIR domain of TIRAP that is available in PDB (3UB2) was used for the molecular docking studies using the ZDOCK server [29]. ZDOCK is a protein-protein docking program that is used to generate rigid-body docking conformations. We used the default parameters of docking, including a blind docking run, to perform a non-biased docking. ZDOCK is a highly validated docking program and has algorithms that are among the best-performing in the Critical Assessment of Prediction of Interactions (CAPRI) [30], a community-wide project assessing the accuracy of protein-protein docking algorithms. Finally, we collected multiple high scoring conformations of the binary complex, of which the best scoring conformation was selected for the molecular dynamics simulation.

The docked complex of c-Jun with TIRAP was subjected to molecular dynamics simulation to determine the stability and structural transition of the complex using the GROMACS 5.1.2 suite [31,32]. Hydrogen atoms were added, and the complex was then settled in a cubic box. The SPC216 water model was used to solvate the box based on periodic boundary conditions. The total charge was neutralized, and the system was minimized by the steepest descent algorithm up to a maximum of 50,000 steps and a convergence tolerance of $1000\ kJ\ mol^{-1}\ nm^{-1}$. The production MD run was carried out for a 100 ns timescale for TIRAP-c-Jun complexes using the protocol described above. The parameters used for the MD simulation can also be found in our previous work [33].

2.9. Computer-assisted screening

A computer-aided virtual screen was performed using the commercially available Discovery Studio 4.3 Program (www.accelrys.com). Only the TIRAP structure from the binary complex was used as the starting point for the screen. An active site grid from the list of sites/spheres was then given by the program. Out of a total of 10 site points that were provided by the program, we found that site 2 encompassed the c-Jun binding site that was identified in the protein-protein docking described above. Hence, we used site 2 for the ligand screening. We utilized the FDA-approved database available in the DrugBank (https://www.drugbank.ca/) for repurposing known drugs with anti-inflammatory activity. The LibDock program in Discovery Studio was used to dock the DrugBank compounds to TIRAP. The docked conformations of the resulting compounds were scored with an intensive scoring analysis using the Score Ligand Poses functionality. Various empirical, force-field and knowledge-based scoring functions (LigScore1-Dreiding and LigScore2-Dreiding) that are implemented in Discovery Studio were used to evaluate the best-docked poses. The resulting poses were automatically saved as SD files and analysed in Discovery Studio. Finally, the compounds were sorted based on the highest (1) LigScore1-Dreiding, (2) LigScore2-Dreiding and (3) LibDock energy scores, as well on their 3-dimensional conformations in the TIRAP binding site.

3. Results

3.1. TIRAP interacts with c-Jun in macrophages in response to LPS stimulation

The initiation and maintenance of the TLR4 signalling transduction pathway requires the adaptor protein TIRAP, which plays an indispensable role in regulating the transactivation of the essential transcription factors NFkB and AP1 [15,34]. Previous studies have described the TIRAP-dependent NFkB p65 transactivation that further amplifies proinflammatory cytokine gene expression [34]. Based purely on these reports, we surmised the involvement of TIRAP in the transactivation of the AP1 transcription factor. To address this possibility, we performed a co-immunoprecipitation (Co-IP) experiment in LPS-stimulated BMDMs. The protein fractions that were prepared from LPS-stimulated macrophages were incubated with either a TIRAP or c-Jun antibody to co-immunoprecipitate the possible interacting proteins, and the immunocomplexes were analysed with anti-c-Jun or anti-TIRAP antibodies. The immunoblot analysis indicated that TIRAP and c-Jun interacted after the stimulation with LPS (Fig. 1A). The relative quantification of the signal intensities obtained from the co-immunoprecipitated blots indicated a statistically significant elevation of the interaction of TIRAP and c-Jun in the presence of LPS (Fig. 1B) compared to that of the controls. The whole cell lysates from LPS-stimulated BMDMs were subjected to Western immunoblotting, and the expression of the total TIRAP and c-Jun was analysed (Fig. 1C). The Co-IP results suggested the presence of a potential interaction between TIRAP and c-Jun, which might play a role in proinflammatory cytokine expression and thereby in the initiation and progression of inflammatory responses.

To further confirm that the two proteins interacted in the endotoxin-induced environment, we performed confocal microscopic analysis. After LPS stimulation, macrophages were stained for TIRAP (Alexa Fluor 594, red) and c-Jun (FITC, green) and visualized by confocal microscopy (Fig. 1D). Compared to those of the control unstimulated macrophages, TIRAP and c-Jun showed increased interaction in macrophages and increased nuclear translocation of AP-1 transcription factor in response to LPS stimulation. The downstream c-Jun activation further provokes the immune machinery in these cells and amplifies the inflammatory response to the LPS/TLR4 signalling.

3.2. Molecular dynamics (MD) simulation of the TIRAP-c-Jun complex

The 3D structure of c-Jun (residues 201 to 256) is not available from the PDB. Hence, we modelled the structure using the Modbase program [28]. The template structure of pre-mRNA-processing-splicing factor 8 had the highest sequence identity of approximately 40% with the query sequence and was selected for homology modelling with the server. The resulting top conformation was retained for the docking run. Molecular docking between c-Jun and TIRAP was performed to understand whether and where the two interact. Hence, a blind docking run was initiated using the ZDOCK server [29], in which we omitted the residue specification to achieve a bias-free relative conformation of the two partners in the complex. The top conformation of the docked complex was used for further analysis. Most of the time, the docking programs accurately predict the docked conformations of the binding partners; however, this is not true every time. Hence, we ran a molecular dynamics simulation of the binary complex to understand and validate the

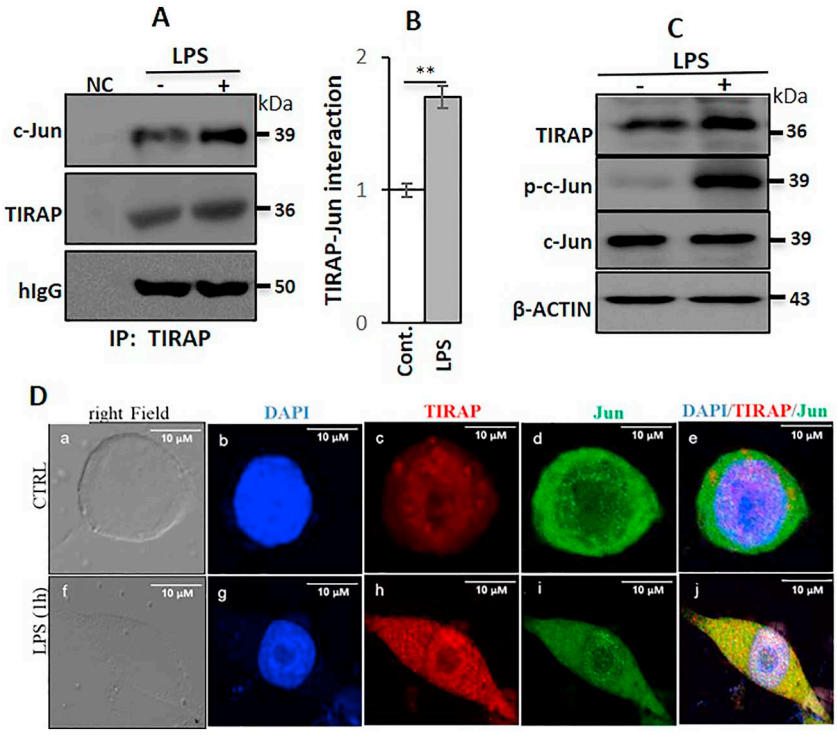

Fig. 1. LPS promotes the TIRAP-c-Jun interaction in macrophages. BMDMs extracted from Swiss albino mice were stimulated with LPS (250 ng/ml) for 1 h. Proteins were harvested and subjected to co-immunoprecipitation (Co-IP) with TIRAP after LPS treatment. (A) Representative immunoblots from Co-IP with (A) TIRAP. (B) Densitometry analysis of the TIRAP-c-Jun interaction. (C) Whole cell lysates from LPS-stimulated BMDMs were subjected to immunoblotting and were resolved by SDS PAGE to analyse the expression of total TIRAP and c-Jun. (D) Confocal microscopy images showing the cellular interaction of TIRAP and c-Jun by staining TIRAP with Alexa Fluor 594-tagged (red) and c-Jun with FITC-tagged (green) secondary antibodies after 1 h of LPS stimulation. All data are representative of three independent experiments and are presented as the mean ± SD, $^{**}P < 0.02$ (Student's *t*-test). (For interpretation of the references to colour in this figure legend, the reader is referred to the web version of this article.)

docking results.

The c-Jun-TIRAP complex was used as a starting point for the MD run. The MD simulations were performed for a long period to fully replicate the original conformations of the complex. The backbone RMSD profile of TIRAP in complex with c-Jun was analysed and is shown in Fig. S1. The TIRAP and c-Jun complexes were well equilibrated after 50 ns of MD production until the end of the simulation, with RMSD values ranging from 1.00 to 1.15 nm. This clearly shows that the complex is consistently stable, as evidenced by the low RMSD difference (1.5 Å) between the initial and final conformations. Further, the residual contribution energy of the TIRAP and c-Jun complex was analysed using MMPBSA calculations. The results show that the residues P71, R81, K84, R115, Y106, R121, R143, K158, Y159, Y187, R192, R200, R207, K210 and R215 of TIRAP and P201 Q203, Q205, Q208, H219, Q218, R221, K226, I245, R252 and K254 of c-Jun have the lowest binding energy and, hence, greatly contribute to the complex stability, as shown in Fig. S2. The lowest energy conformer was retrieved from the trajectory, and its residual interaction analysis showed that residues R192, Q163, E193, M194, E172, L165, Y159, R184 and E190 of TIRAP form stable hydrogen-bond interactions with many c-Jun residues, including E234, Q218, M235, Q203, H219, Q223, Q205, E251, Q214, and E248. In addition, an array of hydrophobic interactions also formed between the TIRAP residues L162, P169, P189, F193, M194, Y195, and Y196 and the c-Jun residues P216, P220, P212, P233, P208, P207, P244, L244, I245, and M235. All of these hydrogen bonds and hydrophobic interactions collectively contribute to the stability of the TIRAP-c-Jun complex. Based on the RMSD and the energy of the complex, along with consistently interacting residues, the TIRAP- c-Jun complex structure seems to be quite stable over time (Supplementary Movie 1), validating our docking model of the TIRAP-c-Jun complex (Fig. 2A & B).

After performing the validation of the complex stability with MD, we initiated a virtual screen against TIRAP. The docking-based virtual screen was carried out using the three-dimensional TIRAP structure. The LibDock program was used, as described above. However, during this analysis, we were careful to select the active site that encompasses the c-Jun binding site. This is because we wanted to target the area on the TIRAP structure that is responsible for c-Jun binding. This would, in turn, enable us to identify compounds binding at the TIRAP site that is meant for c-Jun binding, thereby inhibiting the binary interaction. The

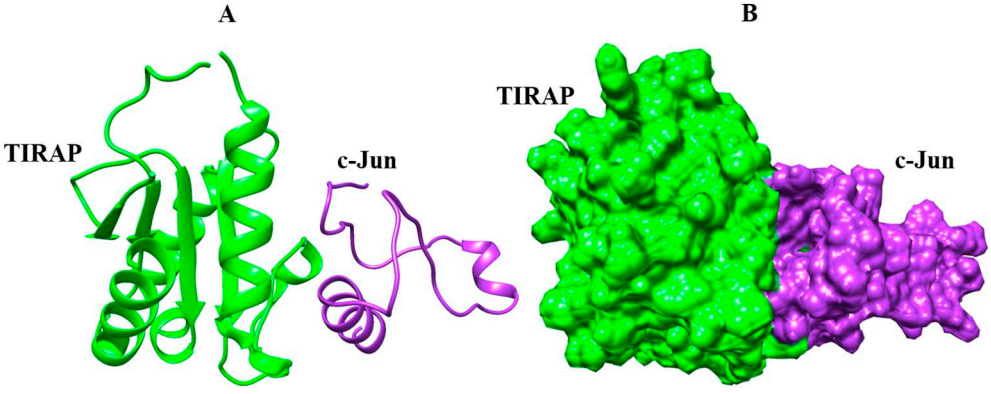

Fig. 2. Docked complex of TIRAP and c-Jun. (A) Ribbon and (B) surface representations of the docked complex of TIRAP (green) and c-Jun (purple). The figure was prepared using UCSF Chimera [52]. (For interpretation of the references to colour in this figure legend, the reader is referred to the web version of this article.)

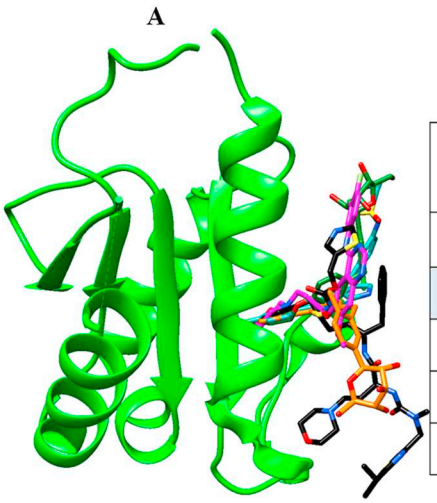

B

Drug	Drug Bank ID	Lig Score1-Drieding	Lig Score2-Drieding	Lib Dock Score
Vemurafenib	DB08881	5.24	4.73	68.35
Gefitinib	DB00317	5.03	4.93	108.25
Cobicistat	DB09065	5.02	6.6	137.53
Empaglifloin	DB09038	5.01	4.88	72.49
Canagliflozin	DB08907	4.98	4.45	63.38

Fig. 3. Docking at the TIRAP-c-Jun interface. (A) Docked conformations of the 5 high-scoring DrugBank compounds: vemurafenib (cyan), gefitinib (magenta), cobicistat (black), empagliflozin (green) and canagliflozin (orange). (B) Docking scores of the selected compounds. The figure was prepared using UCSF Chimera [52]. (For interpretation of the references to colour in this figure legend, the reader is referred to the web version of this article.)

docking run resulted in a total of 9557 confirmations from 1877 drugs deposited in the FDA database. The top conformations of the screened drugs were individually analysed based on their docking energies and binding modes. The docked conformations of these 5 compounds in the TIRAP binding site (meant to bind c-Jun) are shown in Fig. 3. As observed in the figure, all the selected drugs bind TIRAP in an overlapping fashion or in a close vicinity to one another, indicating consistent binding at the TIRAP structure.

3.3. Gefitinib inhibits the TIRAP-c-Jun interaction in LPS-stimulated macrophages

Based on the computational screening, five potential agents (vemurafenib, gefitinib, canagliflozin, empagliflozin, and cobicistat) were identified with a high dock score that inhibited the interface between TIRAP and c-Jun. To validate the in vitro efficacy of the drugs, co-immunoprecipitation was performed using TIRAP and c-Jun antibodies as described previously (Fig. 4A & B). Briefly, BMDMs were stimulated either with LPS alone or with LPS following pre-treatment with the screened drugs. The LPS and drug-treated samples were co-immunoprecipitated with TIRAP and pulled down by agarose beads. An immune complex consisting of a TIRAP antibody was then immunoblotted with c-Jun to examine the modulating effects on the TIRAP-c-Jun interaction. The Co-IP data clearly illustrated that out of the five drugs, gefitinib possessed the maximum blocking effect on the TIRAP-c-Jun interaction. The relative quantification represents the maximum inhibition of the interacting proteins by gefitinib compared to those of the other drugs (Fig. 4B).

To verify that TIRAP and c-Jun interacted, BMDMs were induced with LPS and gefitinib and were subsequently stained with TIRAP and c-Jun antibodies, followed by counterstaining with fluorescent-tagged secondary antibodies (TIRAP-Alexa Fluor 594, red, and c-Jun-FITC, green). Confocal microscopy was used to examine the interaction between the two proteins. The data reveal that unstimulated macrophages do not favour the interaction of the two proteins. However, the addition of LPS to macrophages induces interactions between these two proteins. Further, the confocal analysis from macrophages treated with gefitinib prior to LPS exhibited decreased TIRAP-c-Jun interaction compared to that of the LPS-treated cells (Fig. 4C).

3.4. Gefitinib suppresses the AP1-mediated proinflammatory cytokine expression in LPS-stimulated macrophages

Gefitinib targets the suppression of key inflammatory cytokines, such as IL12, IL23, INF-γ, MIP1-α, M-CSF, and TNF-α, leading to the modulation of the inflammatory reaction (Fig. 5A–F). Quantitative real-time PCR expression analysis revealed an upregulation in cytokine expression with LPS treatment; however, gefitinib pre-treatment suppressed the expression of the cytokines, thereby exhibiting the potential anti-inflammatory activity of gefitinib. Gefitinib is therefore proposed as a potential anti-inflammatory drug that targets the TIRAP and c-Jun interaction, thereby downregulating cytokine expression to suppress the inflammatory cascade.

3.5. Gefitinib exhibits anti-inflammatory properties in endotoxin-induced mice

Mice that were subjected to sepsis with an IP lethal LPS dose (30 mg/kg) were examined for survival when they were injected with gefitinib. All the mice in the control group ($n = 7$ per group) that were injected with the vehicle (DMSO + PBS) alone survived. However, the mice receiving LPS alone showed a 62% mortality rate after 24 h, and the percentage of survival was 15% (85% mortality) at the end of the 72-h period of septic shock (Fig. 6A). In contrast, the group of mice that were injected with gefitinib along with LPS exhibited a higher survival ratio of 76% (24% mortality) after 24 h than that of the LPS group. Interestingly, the survival with gefitinib treatment remained at 69% after 72 h. The survival curve demonstrates the protective efficacy of gefitinib in mice subjected to LPS shock. To study the effect of gefitinib on the lung morphology of LPS-injected mice, lung tissues were harvested, and sections were stained with HE to observe the changes in the healthy tissue. A light microscope was used to capture the morphology at 20× magnification. The control group of mice (DMSO + PBS) had preserved epithelial linings of airways and intact pulmonary capillaries and alveolar septa (Fig. 6B). In contrast, the lungs from septic mice displayed distorted epithelial linings due to the infiltration of neutrophils and lymphocytes. The alveolar septum of the infected mice presented with mucus and a thickened airway lining. In contrast, the lung tissue from the gefitinib pre-treated mice showed a reduction in the damage caused by septic shock. The recovery in gefitinib-injected mice was marked by an intact epithelial lining and normal alveolar septum. Together, these observations demonstrate the protective efficacy of gefitinib in LPS-infected mice, providing a mechanism for therapeutic application.

3.6. Gefitinib treatment attenuates the endotoxin-induced release of cytokines in vivo

The potential anti-inflammatory properties of gefitinib were highlighted in a septic mouse model. Similar to the in vitro data, lung sections from wild-type mice revealed a lack of TIRAP and c-Jun interaction. However, lung tissues from LPS-injected mice demonstrated

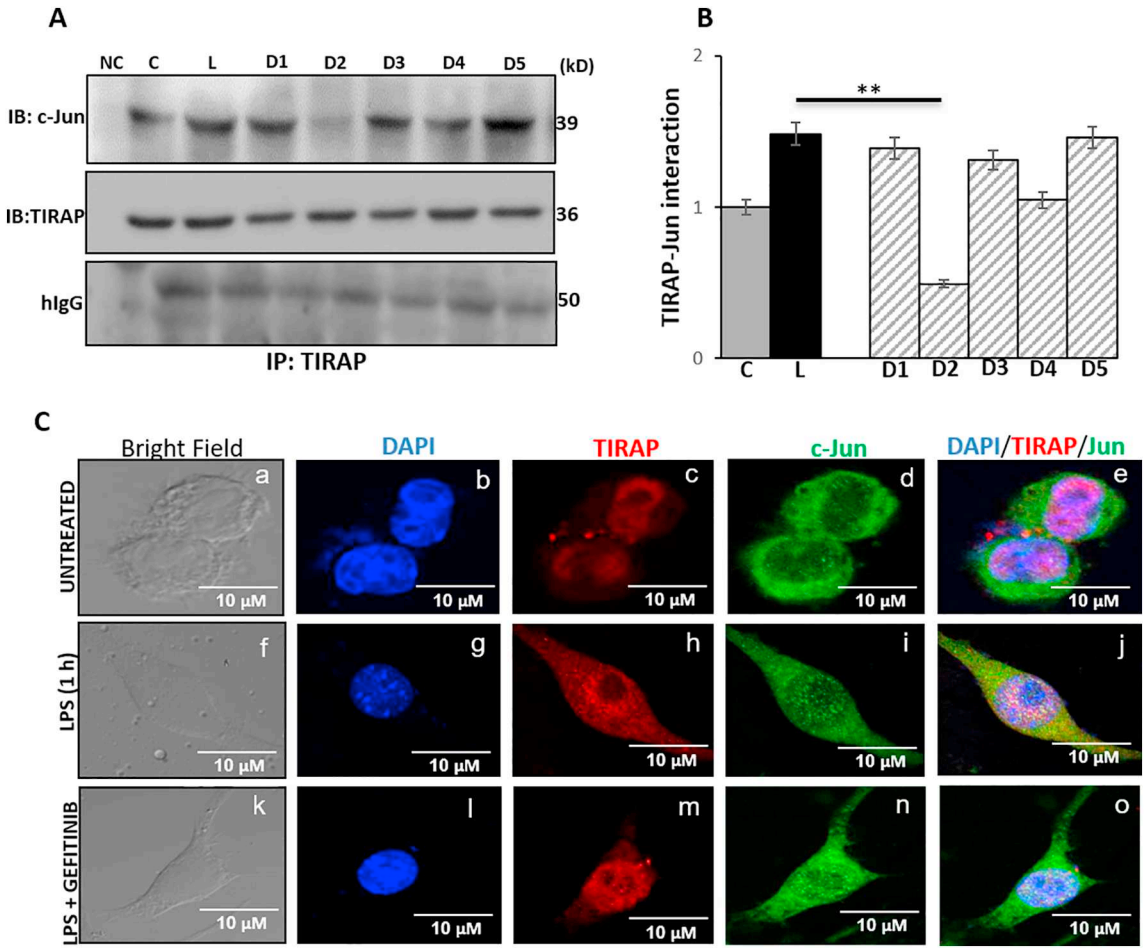

Fig. 4. Among the screened drugs, gefitinib inhibits the TIRAP-c-Jun interaction. BMDMs harvested from Swiss albino mice were treated with LPS (250 ng/ml) in the presence or absence of five drugs (D1: vemurafenib, D2: gefitinib, D3: empagliflozin, D4: canagliflozin and D5: cobicistat) (A) Co-immunoprecipitation with TIRAP and subsequent immunoblotting with c-Jun and TIRAP. (B) Relative quantification of the TIRAP-c-Jun interaction as in (A). (C) Confocal microscopic analysis of BMDMs stimulated with LPS with or without gefitinib after up to 1 h to show the TIRAP and c-Jun interaction. TIRAP was immunostained with an Alexa Fluor 594-tagged secondary antibody (Red) and c-Jun with a FITC-tagged secondary antibody (Green). Nuclei were counterstained with DAPI (blue). All data are representative of three independent experiments and are presented as the mean ± SD, $^{**}P < 0.002$ (Student's *t*-test). (For interpretation of the references to colour in this figure legend, the reader is referred to the web version of this article.)

an interaction between TIRAP and c-Jun. Another group of mice that were pre-treated with gefitinib prior to LPS showed a decrease in the TIRAP and c-Jun interaction compared to that of the LPS group (Fig. 7). Together, the data suggest that gefitinib can impede the TIRAP-c-Jun interaction in the lungs of mice injected with a lethal dose of LPS, and gefitinib is therefore proposed as an anti-inflammatory drug.

To further validate the anti-inflammatory properties of gefitinib, we studied the expression of the AP1-induced cytokines IL12, IL23, INF-γ, MIP1-α, M-CSF and TNF-α in the lung tissue of LPS-injected mice with or without prior gefitinib treatment. In accordance with the previously described LPS-induced cytokine expression, we observed an increase in the cytokines in lung tissue derived from LPS-injected mice compared to those of wild-type mice. Remarkably, in mice that received gefitinib prior to LPS injection, there was a significant reduction in cytokine expression (Fig. 7B–G). The data strongly imply that gefitinib-administered mice failed to produce high levels of inflammatory cytokines and were therefore protected from LPS-induced septic lung injury.

Here, we focused on the AP1-induced inflammatory cytokines that mediate the inflammatory response. Thus, we examined the effect of gefitinib on the expression of the activated AP1 subunit of phospho-c-Jun in the different groups of mice. In contrast to the control mice, mice receiving LPS exhibited elevated expression of phospho-c-Jun, demonstrating the role of AP1 during the LPS-induced inflammatory response. Notably, the expression of phospho-c-Jun was significantly decreased in mice pre-treated with gefitinib prior to LPS (Fig. 7H) compared to that of the LPS group. The quantification of immunoblots showed that gefitinib induced the suppression of phospho-c-Jun expression (Fig. 7I). The results provide a mechanism of gefitinib-induced anti-inflammatory responses in mice.

4. Discussion

Inflammation is a dynamic mechanism that protects the body from the deleterious effects of invading pathogens [35,36]. Signalling events that lead to inflammation arise in immune cells that are activated in response to pathogen recognition [37]. Mammalian Toll-like receptors (TLRs) function as sensors of infection and induce the activation of innate and adaptive immune responses [1,38,39]. Bacterial endotoxin activates the TLR4 signalling pathway and induces sepsis. Evidence suggests that severe endotoxin shock generates a whole-body inflammatory response, leading to multi-organ failure. Lungs are the first organ to demonstrate the apparent damage that is induced during endotoxin shock. Currently, many therapeutic strategies are focused on identifying the protein targets that are essential for overcoming inflammatory lesions that form during endotoxic injury. For instance, studies on bone marrow-derived progenitor cells demonstrate that the

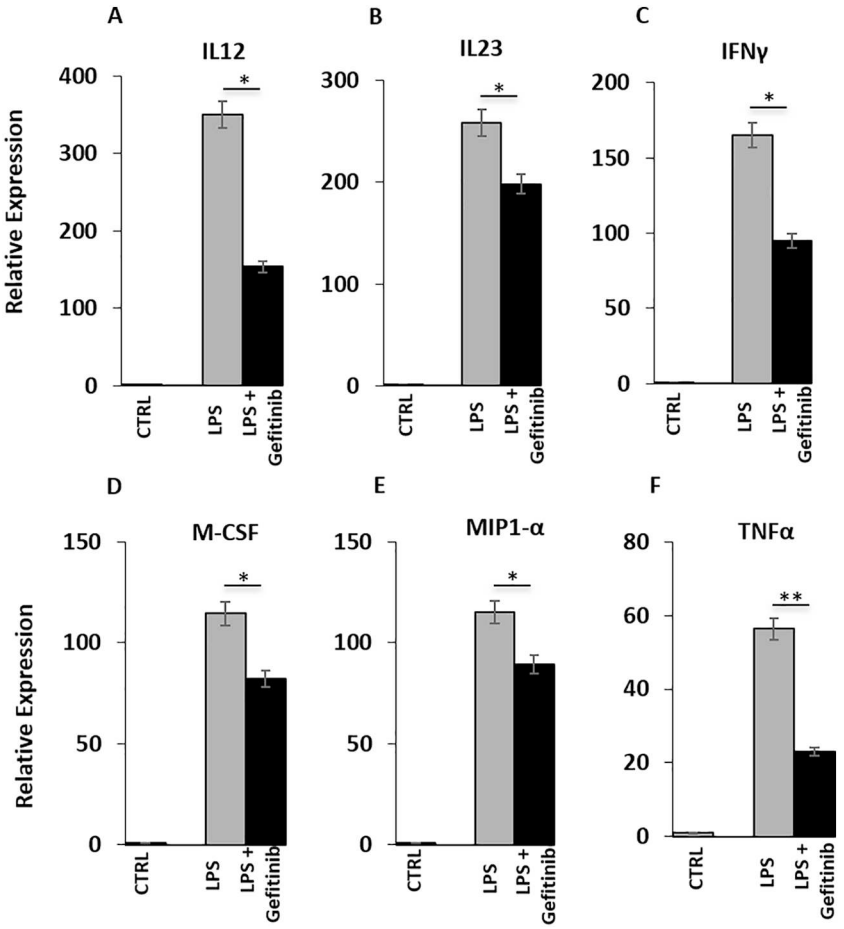

Fig. 5. Gefitinib diminishes the proinflammatory cytokine response of AP1-mediated genes. BMDMs stimulated with LPS (250 ng/ml) in the presence or absence of gefitinib (1 μM) were lysed, and total RNA was extracted. Representative qRT-PCR analysis of the AP1-mediated cytokine mRNA expression of (A) IL12, (B) IL23, (C) IFNγ, (D) MIP1-α, (E) M-CSF and (F) TNF-α normalized to GAPDH. Data are representative of three independent experiments; all data are presented as the mean ± SD. *P* values were determined by a Student's *t*-test, $^{*}P < 0.05$, $^{**}P < 0.005$.

expression of integrins ameliorates LPS-induced lung vascular injury and mouse survival [40]. Therefore, it is of great interest to investigate the molecular targets that regulate the inflammatory cascade in macrophages. Upon recognizing conserved pathogen-associated molecular products, TLRs activate host defence responses through their intracellular signalling domain, the Toll/interleukin-1 receptor (TIR) domain, and the downstream adaptor protein MyD88 [6,41]. TIRAP, an adaptor protein in the TLR signalling pathway, has been identified and has been shown to function downstream of TLR4 [13,42].

In the current study, we observed that TIRAP transactivates c-Jun during LPS shock and hence initiates inflammatory signalling. We investigated the TIRAP-c-Jun interaction with reciprocal coimmunoprecipitation (Fig. 1A & C). Mechanistically, we observed a remarkable increase in the TIRAP and c-Jun interaction in macrophages treated with LPS compared to that of the controls. Increased c-Jun phosphorylation was observed in LPS-stimulated macrophages compared to that of the controls, as indicated in Fig. 1E. We performed confocal analysis to further confirm that TIRAP and c-Jun interacted (Fig. 1F). The interaction between TIRAP and c-Jun suggests that TIRAP-c-Jun complex formation might be an important event in the inflammatory signalling cascade, and that the inhibition of this interaction could protect against the persistent activation of macrophages in chronic inflammatory diseases.

Protein-protein interactions are the convergence and divergence points of many pathways in which they serve positive and/or negative roles in disease progression [43–45]. Similarly, we discovered that the c-Jun-TIRAP interaction is a key event in inflammatory signalling, in which the binary complex triggers a cascade of events leading to the

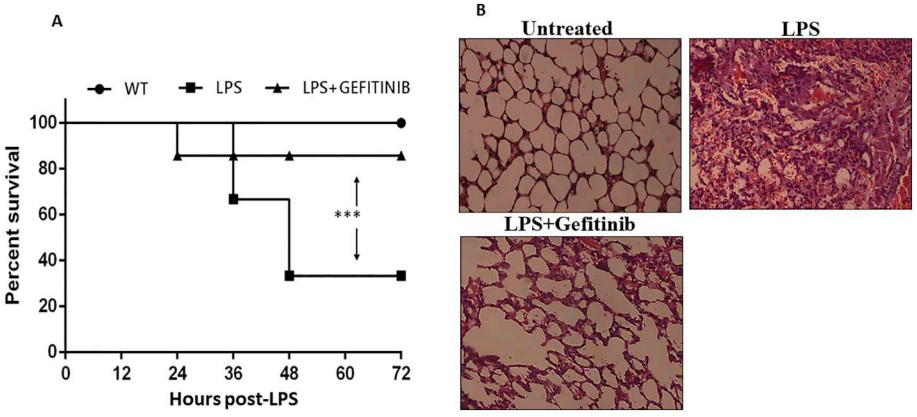

Fig. 6. Gefitinib protects against LPS-induced lung injury in mice. (A) Survival curve of the mice ($n = 14$, each group) treated with LPS alone (20 mg/kg, i.p.) or in combination with gefitinib (40 mg/kg, i.p.) 1 h prior to LPS treatment. (B) Lung histological analyses were performed using haematoxylin and eosin (H&E) staining in the control and gefitinib pretreated mice 8 h after the LPS challenge. Representative images are shown from three mice per phenotype that were analysed in three independent experiments. Scale bar = 100 μm. Significance was determined using Fisher's exact test. **, $P < 0.001$.

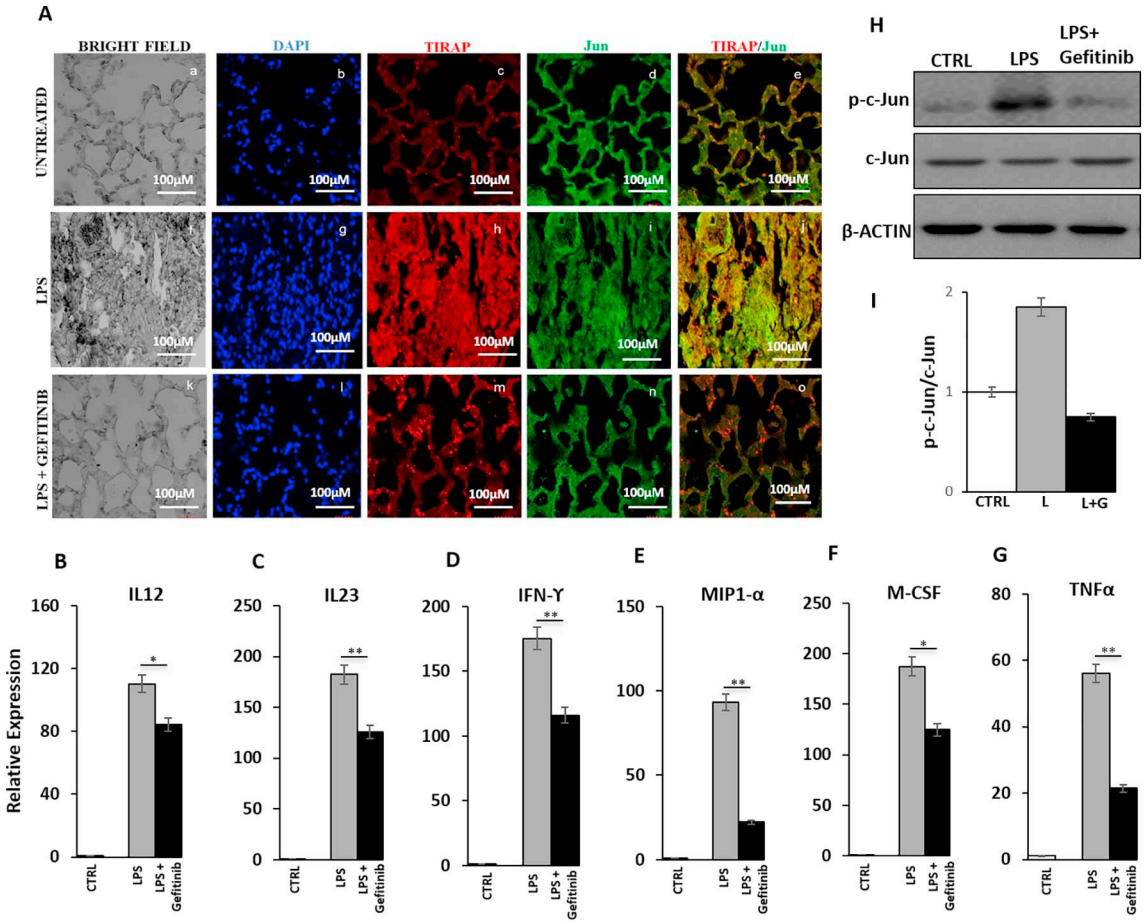

Fig. 7. Gefitinib impedes the TIRAP-c-Jun interaction and the AP1-mediated cytokine gene expression in vivo. Swiss albino mice were challenged with LPS (30 mg/kg) with or without gefitinib (40 mg/kg) 1 h prior to LPS. Lungs were harvested from mice 8 h after LPS and gefitinib treatment. (A) Confocal microscopy images of lung sections stained for TIRAP (Alexa Fluor 594:red) and c-Jun (FITC:green). Nuclei were counterstained with DAPI (blue). Representative qRT-PCR for cytokine mRNA expression from lung tissues for (B) IL12, (C) IL23, (D) IFNγ, (E) MIP1-α, (F) M-CSF and (G) TNF-α normalized to GAPDH. (H) Lung tissues were lysed to measure the protein extraction and were subjected to immunoblotting for phospho-c-jun. (I) Representative densitometric analysis of a phospho-c-Jun immunoblot, as shown in (H). All data are representative of three independent experiments and are presented as the mean ± SD, *P < 0.02, **P < 0.002 (Student's *t*-test). (For interpretation of the references to colour in this figure legend, the reader is referred to the web version of this article.)

release of pro-inflammatory cytokines. We initiated our studies by modelling the c-Jun structure and docking it with TIRAP (Fig. 2A & B). The resulting binary complex was subjected to MD simulations to confirm the docking pose and its stability. The MD RMSD analysis revealed that the TIRAP and c-Jun complex was stabilized by maintaining the backbone fluctuation (Fig. S1). Additionally, the interaction studies of TIRAP and c-Jun clearly show that polar charged and hydrophobic residues contribute to the complex stability, as indicated in Fig. S2. We further utilized the c-Jun binding site on TIRAP to perform virtual screening with an FDA-approved database. The screening was done to repurpose known drugs with the ability to disrupt the c-Jun-TIRAP binary interaction in addition to their original activity/functions against other targets. Drug repurposing has eased the drug discovery process for a little over a decade [46,47]. Drug repurposing has recently gained much popularity owing to its huge applicability and due to the involvement of lower costs and less time. Hence, we used the DrugBank deposited by an FDA-approved database for our studies. Out of the multiple hits that were obtained, we screened the top 5 compounds that showed high binding energy as well as favourable conformation in the c-Jun binding site of TIRAP (Fig. 3A & B).

We tested these drugs in vitro to study their inhibitory potential. Immunoprecipitation was performed with TIRAP and c-Jun in LPS-triggered macrophages in the presence or absence of the drugs (Fig. 4A & B). Among the top 5 drugs selected in silico, only one drug, gefitinib, was found to inhibit the c-Jun-TIRAP interaction in a cell-based assay. Gefitinib exhibits multiple non-covalent interactions with TIRAP that are attributed to its high scoring and snug fitting conformation in the TIRAP binding site, as demonstrated in Supplementary Fig. 3. We next performed confocal analysis and confirmed the inhibitory potential of gefitinib in vitro, as shown in Fig. 4C. We further examined the AP-1-mediated pro-inflammatory cytokine expression, which clearly shows that gefitinib treatment prior to LPS stimulation significantly reduces cytokine expression compared to that of LPS-treated macrophages (Fig. 5).

Gefitinib is currently used to treat a specific subset of breast, lung and other cancers [48–51]. Here, we report a unique mechanism utilized by gefitinib to suppress inflammatory cascade in macrophages. We further determined the in vivo efficacy of gefitinib in mice that were treated with LPS. Mice administered gefitinib prior to LPS treatment exhibited remarkable recovery from endotoxin shock and showed increased survival compared to that of the LPS-injected mice (Fig. 6). The microscopic examination of the lung morphology from the same group of mice suggests that gefitinib protected the mice from LPS-induced lung injury. Real-time PCR analyses also measured the cytokine increases in the lungs of septic mice, which is consistent with the survival data (Fig. 7B–G). Importantly, the LPS-treated group displayed a higher expression level of inflammatory cytokines compared to the gefitinib-treated group. The data suggest that gefitinib is a potent anti-

inflammatory agent that can be utilized in chronic (or acute) inflammatory disorders.

Supplementary data to this article can be found online at https://doi.org/10.1016/j.intimp.2019.03.031.

Acknowledgments

The authors are thankful to the Department of Biotechnology (DBT) of the Government of India that sponsored the Ramalingaswami Fellowship of MSB (BT/RLF/Re-entry/26/2013). The authors are thankful to the Department of Science and Technology (DST) of the Government of India for providing financial support under the Early Career Research (ECR) Award (ECR/2016/00852) of MSB. The authors are thankful to Choithram Hospital and Research Centre (CHRC) for providing us with the facility to perform tissue sectioning and staining. The authors also gratefully acknowledge the Indian Institute of Technology Indore (IITI) for providing facilities and other support.

Contributions

M.S.B. conceived and designed the research; M.S., U.S., B.K.; and K.M. conducted the research; all authors analysed the data; M.S.B. wrote the manuscript; and S.B. and K.W. edited and reviewed the manuscript.

Competing interests

The authors declare no competing interests.

References

[1] S.K. Drexler, B.M. Foxwell, The role of toll-like receptors in chronic inflammation, Int. J. Biochem. Cell Biol. 42 (2010) 506–518, https://doi.org/10.1016/j.biocel.2009.10.009.
[2] Y. Lu, X. Li, S. Liu, Y. Zhang, D. Zhang, Toll-like receptors and inflammatory bowel disease, Front. Immunol. 9 (2018), https://doi.org/10.3389/fimmu.2018.00072.
[3] Y. Lai, R.L. Gallo, Toll-like receptors in skin infectious and inflammatory diseases, Infect. Disord. Drug Targets 8 (2008) 144–155.
[4] S. Janssens, R. Beyaert, Role of toll-like receptors in pathogen recognition, Clin. Microbiol. Rev. 16 (2003) 637–646, https://doi.org/10.1128/CMR.16.4.637-646.2003.
[5] L. Yu, L. Wang, S. Chen, Endogenous toll-like receptor ligands and their biological significance, J. Cell. Mol. Med. 14 (2010) 2592–2603, https://doi.org/10.1111/j.1582-4934.2010.01127.x.
[6] J. Deguine, G.M. Barton, MyD88: a central player in innate immune signaling, F1000Prime Rep. 6 (2014), https://doi.org/10.12703/P6-97.
[7] T. Kawasaki, T. Kawai, Toll-like receptor signaling pathways, Front. Immunol. 5 (2014), https://doi.org/10.3389/fimmu.2014.00461.
[8] J. Sakai, E. Cammarota, J.A. Wright, P. Cicuta, R.A. Gottschalk, N. Li, I.D.C. Fraser, C.E. Bryant, Lipopolysaccharide-induced NF-κB nuclear translocation is primarily dependent on MyD88, but TNFα expression requires TRIF and MyD88, Sci. Rep. 7 (2017), https://doi.org/10.1038/s41598-017-01600-y.
[9] M. Yamamoto, S. Sato, H. Hemmi, K. Hoshino, T. Kaisho, H. Sanjo, O. Takeuchi, M. Sugiyama, M. Okabe, K. Takeda, S. Akira, Role of adaptor TRIF in the MyD88-independent toll-like receptor signaling pathway, Science 301 (2003) 640–643, https://doi.org/10.1126/science.1087262.
[10] B. Verstak, K. Nagpal, S.P. Bottomley, D.T. Golenbock, P.J. Hertzog, A. Mansell, MyD88 adapter-like (mal)/TIRAP interaction with TRAF6 is critical for TLR2- and TLR4-mediated NF-κB proinflammatory responses, J. Biol. Chem. 284 (2009) 24192–24203, https://doi.org/10.1074/jbc.M109.023044.
[11] E. Andreakos, S.M. Sacre, C. Smith, A. Lundberg, S. Kiriakidis, T. Stonehouse, C. Monaco, M. Feldmann, B.M. Foxwell, Distinct pathways of LPS-induced NF-kappa B activation and cytokine production in human myeloid and nonmyeloid cells defined by selective utilization of MyD88 and Mal/TIRAP, Blood 103 (2004) 2229–2237, https://doi.org/10.1182/blood-2003-04-1356.
[12] N.J. Bernard, L.A. O'Neill, Mal, more than a bridge to MyD88, IUBMB Life 65 (2013) 777–786, https://doi.org/10.1002/iub.1201.
[13] T. Horng, G.M. Barton, R. Medzhitov, TIRAP: an adapter molecule in the Toll signaling pathway, Nat. Immunol. 2 (2001) 835–841, https://doi.org/10.1038/ni0901-835.
[14] T. Horng, G.M. Barton, R.A. Flavell, R. Medzhitov, The adaptor molecule TIRAP provides signalling specificity for Toll-like receptors, Nature 420 (2002) 329–333, https://doi.org/10.1038/nature01180.
[15] M.S. Baig, D. Liu, K. Muthu, A. Roy, U. Saqib, A. Naim, S.M. Faisal, M. Srivastava, R. Saluja, Heterotrimeric complex of p38 MAPK, PKCδ, and TIRAP is required for AP1 mediated inflammatory response, Int. Immunopharmacol. 48 (2017) 211–218, https://doi.org/10.1016/j.intimp.2017.04.028.
[16] K.A. Fitzgerald, E.M. Palsson-McDermott, A.G. Bowie, C.A. Jefferies, A.S. Mansell, G. Brady, E. Brint, A. Dunne, P. Gray, M.T. Harte, D. McMurray, D.E. Smith, J.E. Sims, T.A. Bird, L.A. O'Neill, Mal (MyD88-adapter-like) is required for Toll-like receptor-4 signal transduction, Nature 413 (2001) 78–83, https://doi.org/10.1038/35092578.
[17] P. Gray, A. Dunne, C. Brikos, C.A. Jefferies, S.L. Doyle, L.A.J. O'Neill, MyD88 adapter-like (Mal) is phosphorylated by Bruton's tyrosine kinase during TLR2 and TLR4 signal transduction, J. Biol. Chem. 281 (2006) 10489–10495, https://doi.org/10.1074/jbc.M508892200.
[18] W. Piao, C. Song, H. Chen, L.M. Wahl, K.A. Fitzgerald, L.A. O'Neill, A.E. Medvedev, Tyrosine phosphorylation of MyD88 adapter-like (Mal) is critical for signal transduction and blocked in endotoxin tolerance, J. Biol. Chem. 283 (2008) 3109–3119, https://doi.org/10.1074/jbc.M707400200.
[19] M.S. Baig, S.V. Zaichick, M. Mao, A.L. de Abreu, F.R. Bakhshi, P.C. Hart, U. Saqib, J. Deng, S. Chatterjee, M.L. Block, S.M. Vogel, A.B. Malik, M.E.L. Consolaro, J.W. Christman, R.D. Minshall, B.N. Gantner, M.G. Bonini, NOS1-derived nitric oxide promotes NF-κB transcriptional activity through inhibition of suppressor of cytokine signaling-1, J. Exp. Med. 212 (2015) 1725–1738, https://doi.org/10.1084/jem.20140654.
[20] T. Curran, B.R. Franza, Fos and Jun: the AP-1 connection, Cell 55 (1988) 395–397.
[21] J. Hess, P. Angel, M. Schorpp-Kistner, AP-1 subunits: quarrel and harmony among siblings, J. Cell Sci. 117 (2004) 5965–5973, https://doi.org/10.1242/jcs.01589.
[22] M. Gustems, A. Woellmer, U. Rothbauer, S.H. Eck, T. Wieland, D. Lutter, W. Hammerschmidt, c-Jun/c-Fos heterodimers regulate cellular genes via a newly identified class of methylated DNA sequence motifs, Nucleic Acids Res. 42 (2014) 3059–3072, https://doi.org/10.1093/nar/gkt1323.
[23] T.K. Kerppola, T. Curran, Fos-Jun heterodimers and Jun homodimers bend DNA in opposite orientations: implications for transcription factor cooperativity, Cell 66 (1991) 317–326.
[24] C.E. Malnou, F. Brockly, C. Favard, G. Moquet-Torcy, M. Piechaczyk, I. Jariel-Encontre, Heterodimerization with different Jun proteins controls c-Fos intranuclear dynamics and distribution, J. Biol. Chem. 285 (2010) 6552–6562, https://doi.org/10.1074/jbc.M109.032680.
[25] R. Wisdom, AP-1: one switch for many signals, Exp. Cell Res. 253 (1999) 180–185, https://doi.org/10.1006/excr.1999.4685.
[26] K. Chida, S. Nagamori, T. Kuroki, Nuclear translocation of Fos is stimulated by interaction with Jun through the leucine zipper, Cell. Mol. Life Sci. 55 (1999) 297–302, https://doi.org/10.1007/s000180050291.
[27] M. Srivastava, M.S. Baig, NOS1 mediates AP1 nuclear translocation and inflammatory response, Biomed. Pharmacother. 102 (2018) 839–847, https://doi.org/10.1016/j.biopha.2018.03.069.
[28] U. Pieper, B.M. Webb, G.Q. Dong, D. Schneidman-Duhovny, H. Fan, S.J. Kim, N. Khuri, Y.G. Spill, P. Weinkam, M. Hammel, J.A. Tainer, M. Nilges, A. Sali, ModBase, a database of annotated comparative protein structure models and associated resources, Nucleic Acids Res. 42 (2014) D336–D346, https://doi.org/10.1093/nar/gkt1144.
[29] B.G. Pierce, K. Wiehe, H. Hwang, B.-H. Kim, T. Vreven, Z. Weng, ZDOCK server: interactive docking prediction of protein-protein complexes and symmetric multimers, Bioinformatics 30 (2014) 1771–1773, https://doi.org/10.1093/bioinformatics/btu097.
[30] J. Janin, K. Henrick, J. Moult, L.T. Eyck, M.J.E. Sternberg, S. Vajda, I. Vakser, S.J. Wodak, Critical assessment of PRedicted interactions, CAPRI: a critical assessment of PRedicted interactions, Proteins 52 (2003) 2–9, https://doi.org/10.1002/prot.10381.
[31] B. Hess, C. Kutzner, D. van der Spoel, E. Lindahl, GROMACS 4: algorithms for highly efficient, load-balanced, and scalable molecular simulation, J. Chem. Theory Comput. 4 (2008) 435–447, https://doi.org/10.1021/ct700301q.
[32] D. Van Der Spoel, E. Lindahl, B. Hess, G. Groenhof, A.E. Mark, H.J.C. Berendsen, GROMACS: fast, flexible, and free, J. Comput. Chem. 26 (2005) 1701–1718, https://doi.org/10.1002/jcc.20291.
[33] K. Muthu, M. Panneerselvam, N.S. Topno, M. Jayaraman, K. Ramadas, Structural perspective of ARHI mediated inhibition of STAT3 signaling: an insight into the inactive to active transition of ARHI and its interaction with STAT3 and importinβ, Cell. Signal. 27 (2015) 739–755, https://doi.org/10.1016/j.cellsig.2014.11.036.
[34] A. Mansell, R. Smith, S.L. Doyle, P. Gray, J.E. Fenner, P.J. Crack, S.E. Nicholson, D.J. Hilton, L.A.J. O'Neill, P.J. Hertzog, Suppressor of cytokine signaling 1 negatively regulates Toll-like receptor signaling by mediating Mal degradation, Nat. Immunol. 7 (2006) 148–155, https://doi.org/10.1038/ni1299.
[35] R. Medzhitov, Origin and physiological roles of inflammation, Nature (2008), https://doi.org/10.1038/nature07201.
[36] U. Weiss, Inflammation, Nature (2008), https://doi.org/10.1038/454427a.
[37] K. Newton, V.M. Dixit, Signaling in innate immunity and inflammation, Cold Spring Harb. Perspect. Biol. 4 (2012), https://doi.org/10.1101/cshperspect.a006049.
[38] S. Akira, K. Takeda, Toll-like receptor signalling, Nat. Rev. Immunol. 4 (2004) 499–511, https://doi.org/10.1038/nri1391.
[39] S. Akira, K. Takeda, T. Kaisho, Toll-like receptors: critical proteins linking innate and acquired immunity, Nat. Immunol. 2 (2001) 675–680, https://doi.org/10.1038/90609.
[40] K.K. Wary, S.M. Vogel, S. Garrean, Y.D. Zhao, A.B. Malik, Requirement of alpha(4) beta(1) and alpha(5)beta(1) integrin expression in bone-marrow-derived progenitor cells in preventing endotoxin-induced lung vascular injury and edema in mice, Stem Cells 27 (2009) 3112–3120, https://doi.org/10.1002/stem.241.
[41] K.B. Narayanan, H.H. Park, Toll/interleukin-1 receptor (TIR) domain-mediated cellular signaling pathways, Apoptosis 20 (2015) 196–209, https://doi.org/10.1007/s10495-014-1073-1.

[42] M. Yamamoto, S. Sato, H. Hemmi, H. Sanjo, S. Uematsu, T. Kaisho, K. Hoshino, O. Takeuchi, M. Kobayashi, T. Fujita, K. Takeda, S. Akira, Essential role for TIRAP in activation of the signalling cascade shared by TLR2 and TLR4, Nature 420 (2002) 324–329, https://doi.org/10.1038/nature01182.
[43] M.W. Gonzalez, M.G. Kann, Chapter 4: protein interactions and disease, PLoS Comput. Biol. 8 (2012), https://doi.org/10.1371/journal.pcbi.1002819.
[44] U. Kuzmanov, A. Emili, Protein-protein interaction networks: probing disease mechanisms using model systems, Genome Med. 5 (2013) 37, https://doi.org/10.1186/gm441.
[45] S. Petrakis, M.A. Andrade-Navarro, Editorial: protein interaction networks in health and disease, Front. Genet. 7 (2016), https://doi.org/10.3389/fgene.2016.00111.
[46] S.M. Corsello, J.A. Bittker, Z. Liu, J. Gould, P. McCarren, J.E. Hirschman, S.E. Johnston, A. Vrcic, B. Wong, M. Khan, J. Asiedu, R. Narayan, C.C. Mader, A. Subramanian, T.R. Golub, The Drug Repurposing Hub: a next-generation drug library and information resource, Nat. Med. 23 (2017) 405–408, https://doi.org/10.1038/nm.4306.
[47] N. Nosengo, Can you teach old drugs new tricks? Nature 534 (2016) 314–316, https://doi.org/10.1038/534314a.
[48] A. Barker, D. Andrews, Chapter 8 - discovery and development of the anticancer agent gefitinib, an inhibitor of the epidermal growth factor receptor tyrosine kinase, in: R. Ganellin, S. Roberts, R. Jefferis (Eds.), Introd. Biol. Small Mol. Drug Res. Dev. Elsevier, Oxford, 2013, pp. 255–281, , https://doi.org/10.1016/B978-0-12-397176-0.00008-X.
[49] D. Geng, D. Sun, L. Zhang, W. Zhang, The therapy of gefitinib towards breast cancer partially through reversing breast cancer biomarker arginine, Afr. Health Sci. 15 (2015) 594–597, https://doi.org/10.4314/ahs.v15i2.36.
[50] N. Moryl, E.A. Obbens, O.H. Ozigbo, M.G. Kris, Analgesic effect of gefitinib in the treatment of non-small cell lung cancer, J. Support. Oncol. (4) (2006) 111.
[51] M. Muhsin, J. Graham, P. Kirkpatrick, Gefitinib, Nat. Rev. Drug Discov. 2 (2003) 515–516, https://doi.org/10.1038/nrd1136.
[52] E.F. Pettersen, T.D. Goddard, C.C. Huang, G.S. Couch, D.M. Greenblatt, E.C. Meng, T.E. Ferrin, UCSF Chimera-a visualization system for exploratory research and analysis, J. Comput. Chem. 25 (13) (2004) 1605–1612, https://doi.org/10.1002/jcc.20084.